Uranyl complexes formed with a *para-t*-butylcalix[4]arene bearing phosphinoyl pendant arms on the lower rim. Solid and solution studies

By F. de M. Ramírez[1,*], S. Varbanov[2], J.-C. G. Bünzli[3], J. F. Rivas-Silva[4], M. A. Ocaña-Bribiesca[4], M. A. Cortés-Jácome[5] and J. A. Toledo-Antonio[5]

[1] Instituto Nacional de Investigaciones Nucleares, Departamento de Química, Carretera México-Toluca S/N. La Marquesa, Ocoyoacac, C.P. 52750, México
[2] Institute of Organic Chemistry with Center of Phytochemistry, Bulgarian Academy of Sciences, 1113 Sofia, Bulgaria
[3] École polytechnique Fédérale de Lausanne (EPFL). Institute of Chemical Sciences and Engineering, BCH 1402, 1015 Lausanne, Switzerland
[4] Instituto de Física de la BUAP, Apdo. Postal J-48, Puebla, Puebla 72570, México
[5] Instituto Mexicano del Petróleo/Programa de Ingeniería Molecular, Eje Central Lázaro Cárdenas 152, D.F., 7730, México

Summary. The current interest in functionalized calixarenes with phosphorylated pendant arms resides in their coordination ability towards f elements and capability towards actinide/rare earth separation. Uranyl cation forms 1 : 1 and 1 : 2 (M : L) complexes with a tetra-phosphinoylated *p-tert*-butylcalix[4]arene, B_4bL^4: $UO_2(NO_3)_2(B_4bL^4)_n \cdot xH_2O$ ($n = 1$, $x = 2$, **1**; $n = 2$, $x = 6$, **2**). Spectroscopic data point to the inner coordination sphere of **1** containing one monodentate nitrate anion, one water molecule and the four phosphinoylated arms bound to UO_2^{2+} while in **2**, uranyl is only coordinated to calixarene ligands. In both cases the U(VI) ion is 8-coordinate. Uranyl complexes display enhanced metal-centred luminescence due to energy transfer from the calixarene ligands; the luminescence decays are bi-exponential with associated lifetimes in the ranges $220\,\mu s < \tau_s < 250\,\mu s$ and $630\,\mu s < \tau_L < 640\,\mu s$, pointing to the presence of two species with differently coordinated calixarene, as substantiated by a XPS study of U($4f_{5/2,7/2}$), O($1s$) and P($2p$) levels on solid state samples. The extraction study of UO_2^{2+} cation and trivalent rare-earth (Y, La, Eu) ions from acidic nitrate media by B_4bL^4 in chloroform shows the uranyl cation being much more extracted than rare earths.

1. Introduction

In general, the development of actinide (An) coordination chemistry has been somewhat limited in view of high radiotoxicity and the very small quantities available for some of the radioisotopes. Complexes with weakly α-emitting, long half-life radio-elements such as uranium [1–7] and tetravalent thorium [1, 6, 7] have been the most studied while lan-

thanide ions (Ln), in an indirect way, have afforded knowledge on the chemical behaviour of trivalent actinides [7, 8].

Physicochemical properties of simple uranyl compounds have been widely studied in aqueous solution [4, 9, 10], in organic solvents [6, 10–12], and in the solid state [13, 14]. Semi-empirical [15, 16] and first-principles studies [17] have been essential to decipher the electronic and vibronic states, the nature of the chemical bonds in uranyl coordination compounds [18–20], as well as to model extraction mechanisms [21]. For instance, DFT calculations of complexes with carboxylic [18], aromatic [19], and hydroxamic acids [20] are in good agreement with experimental data such as stability constants, structural parameters derived from X-ray or EXAFS experiments, and spectroscopic properties.

The calixarene impact in different fields of science and technology has been reviewed very recently [22–24 and references cited in].

Since the nineties, a large interest has developed for the interaction between f elements and properly functionalized calixarenes, in particular, in the hope of designing adequate systems from their selective extraction and for An/Ln separation. In particular, calixarenes fitted with pendant arms containing groups such as phosphoryl and/or amide have proved to display powerful extraction ability and large selectivity [6, 25–31]. Effectiveness of these macrocycles in the treatment of radioactive wastes containing lanthanides, actinides, alkaline, and alkaline earths has been practically demonstrated [22–24, 28, 31, 32]. Calixarenes complexes with uranyl revealed to be quite stable [6, 33] but few phosphorylated calixarenes have been tested for uranyl extraction [6, 27, 30, 31].

With this in mind, we have been involved during the past years in the synthesis of two series of calix[n]arenes ($n = 4$, 6, 8; see Fig. 1a) fitted with ether amide [34, 35] and phosphinoyl pendant arms [6, 36–38] on the narrow rim. We have reported the structural and photophysical properties of their

*Author for correspondence
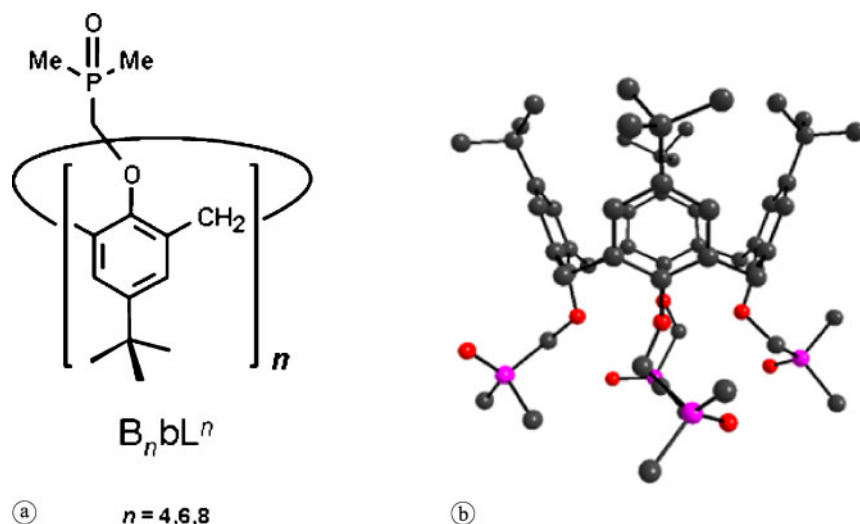(E-mail: flor.ramirez@inin.gob.mx, jean-claude.bunzli@epfl.ch).

Fig. 1. (**a**) Calixarenes with phosphinoyl pendant arms in the lower rims, (**b**) tetra-phosphinoylated *p-tert*-butylcalix[4]arene, B_4bL^4. Hydrogen atoms are not shown for clarity.

lanthanide complexes [34–38]. Recently, our work has been expanded to the study of actinide complexes formed with the phosphinoyl-derivatized calix[6]arene B_6bL^6, as well as to its extraction capability towards uranyl, thorium(IV), and representative trivalent rare earths (Y, La, Eu) [6]. The synergistic effect of the phosphinoyl-derivatized calix[4]arene B_4bL^4 (Fig. 1b) in the extraction of lanthanides with a pyrazolone derivative has also been shortly reported by one of us [39]. In the continuation of these studies, we report here on the coordination ability of B_4bL^4 towards uranyl cations with the characterization of the resulting 1 : 1 and 1 : 2 complexes through several spectroscopic techniques, including XPS, backed by model calculations. We also present the extraction properties of B_4bL^4 with respect to uranyl and uranyl/rare earth separation in three different aqueous media.

2. Experimental procedures

$UO_2(NO_3)_2 \cdot 6H_2O$, ethanol and di-isopropyl ether were purchased from Merck. Nitric acid (purity 65.1%, specific density 1.3989), formic acid (purity, 90%), sodium formate and nitrate were from Baker. De-ionized water was kindly supplied by the staff of the Nuclear Reactor TRIGA Mark III from the Nuclear Centre of Mexico. Anhydrous (< 0.005% water) chloroform, acetonitrile, diethyl ether, as well as spectroscopic grade dichloromethane, acetonitrile, and Arsenazo III were purchased from Aldrich and used without further purification or dehydration. The lower-rim substituted *p-tert*-butylcalix[4]arene B_4bL^4 (5,11,17,23-tetra-*tert*-butyl-25,26,27,28-tetrakis (dimethyl-phosphinoylmethoxy)-calix[4]arene), was obtained as reported previously [36].

2.1 Synthesis of the uranyl complexes

The hygroscopic 1 : 1 and 1 : 2 uranyl complexes, **1** and **2** compounds, respectively, were prepared according to the procedure reported recently for B_6bL^6 [6].

1 : 1 complexes

A solution of $UO_2(NO_3)_2 \cdot 6H_2O$ (0.1 mmol), in 2 cm³ EtOH was heated at 45 °C and 0.1 mmol of L = B_4bL^4 in 4 cm³ EtOH was added dropwise. The mixture was stirred 1 h at

45 °C and then 5 h under N_2 atmosphere at room temperature (RT, 291 ± 2 K). Precipitation was induced by evaporating half of the solvent, or without evaporation by addition of diethyl or di-isopropyl ether until the solution turned turbid; it was then left overnight at −20 °C. The hygroscopic precipitates were separated by centrifugation and washed three times with 8 cm³ EtOH and dried for 20 h at 40 °C and for 72 h at 80 °C under reduced pressure at 933 Pa. Compound **1** was greenish.

1 : 2 complexes

A solution of $UO_2(NO_3)_2 \cdot 6H_2O$ (0.06 mmol) in 3 cm³ dry CH_3CN was added dropwise to a solution of 0.1 mmol of B_4bL^4 in 25 cm³ of dry CH_3CN heated at 45 °C. The resulting mixture was stirred for 5 h under N_2 atmosphere at this temperature and one additional hour without heating. The solvent was half evaporated and replaced by diisopropyl ether until the solution turned turbid (45 cm³). The precipitate was centrifuged, washed with diisopropyl ether and dried for 20 h at 40 °C and for 72 h at 80 °C under reduced pressure at 933 Pa. Compound **2** was greenish.

2.2 Characterization of the uranyl complexes

Due to the hygroscopic nature of the calixarene and the complexes, IR spectra were recorded after heating the KBr disk at 95 °C for 25 h. Diffuse reflectance (DR) spectra were recorded in MgO without drying the pellets. UV-Vis and luminescence spectra were recorded in dried CH_3CN. NMR spectra in CD_3CN. For comparison calixarene B_4bL^4 was characterized by the same techniques than the synthesized complexes. IR (cm⁻¹) $v(P-CH_3)$, 1297; $v(P=O)$, 1196, 1172; $v(=C-O-CH_2-)$, 1018; $vH_2O_{lattice}$, 555, 522, 494, 356. DR, ($\pi \to \pi^*$ transitions, cm⁻¹): P=O, 42 020 (238 nm); $-C=C_{phenyl}$, 35 335 (283 nm). UV-Vis, λ_{max} 275 nm; ε (M⁻¹ cm⁻¹): 3780. NMR, δ (ppm): ¹H NMR, 7.09 (8 H, s, H_{arom}), 4.84 (4 H, d, $J = 12.96$ Hz, $CH_{2\,ax}$-calix); 4.66 (8 H, d, $J_{H-P} = 1.93$ Hz, CH_2-arm); 3.32 (4 H, d, $J = 13.01$ Hz, $CH_{2\,eq}$-calix); 2.0–2.55 (4 H, free H_2O); 1.45 (24 H, d, $J_{H-P} = 13.38$ Hz, CH_3-arm); 1.16 (36 H, s, H-*t*-Bu). ³¹P{¹H} NMR, 37.390; ¹³C{¹H} NMR, CH_3-P (15.80, 15.27); CH_2-ring (31.68); $C(CH_3)_3$

(34.75); CH_2–P (74.85, 75.47); CH (126.78); $C(CH_3)_3$ (134.75, 147.04).

Compound 1

Reaction yield: 56%. Elemental analysis: [found: C, 46.27; H, 6.23; N, 2.01, %. Calc. for $UO_2(B_4bL^4)(NO_3)_2$·$2H_2O$, $C_{56}H_{88}N_2O_{18}P_4U$: C, 46.73; H, 6.16; N, 1.95, %]. IR (cm^{-1}): v(P–CH_3), 1300; v(P=O), 1193; v(=C–O–CH_2–), 1024; v(O=U=O), 915$_{strong}$; $vNO_{3\,ionic}$ 1384, $vNO_{3\,monocoord}$ 1540, 1521, 767; $vH_2O_{lattice}$, 553, 523, 356; vH_2O_{coord}, 504, 380. DR, ($\pi \to \pi^*$ transitions, cm^{-1}): P=O, 44 845 (223 nm); –C=C$_{phenyl}$, 33 005 (303 nm). UV-Vis, λ_{max} 275 nm; ε (M^{-1} cm^{-1}): 4140. NMR, δ (ppm): ^1H NMR, 7.16 (8 H, broad, H_{arom}); 4.72 (4.1–5.7) (10 H, very broad, $CH_{2\,ax}$-calix and CH_2-arm); 3.44 (3.2–4.1) (4 H, broad, $CH_{2\,eq}$-calix); (2.2–3.1) (2 H, free H_2O); 1.63 (9 H, broad), 1.29 (9 H, s, relatively sharp), 0.91 (3 H, t, $J_{H-P} = 6.28$ Hz), $(CH_3)_2PO$); 1.17 (36 H, broad, H-*t*-Bu). $^{31}P\{^1H\}$ NMR, 37.392, 37.391. $^{13}C\{^1H\}$ NMR, CH_3-P (12.52,11.22); CH_2-ring (31.63); CH_2–P (77.70).

Compound 2

Reaction yield: 68%. Elemental analysis: [found: C, 52.70; H, 7.25; N, 1.24, %. Calc. for $UO_2(B_4bL^4)_2(NO_3)_2$·$6H_2O$, $C_{112}H_{180}N_2O_{30}P_8U$: C, 53.37; H, 7.20; N, 1.11, %]. IR (cm^{-1}): v(P–CH_3), 1300 v(P=O), 1194, 1173; v(=C–OCH_2–), 1024; v(O=U=O), 916$_{whoulder}$; $vNO_{3\,ionic}$, 1384; $vH_2O_{lattice}$, 356. DR, ($\pi \to \pi^*$ transitions, cm^{-1}), 35 715 cm^{-1} (280 nm). UV-Vis, λ_{max} 275 nm; ε (M^{-1} cm^{-1}), 6700. NMR, δ (ppm): ^1H NMR, 8.51 (1H, hydrogen bonded water to OP); 7.16 (16 H very broad, asymmetric, H_{arom}); 4.73 (20 H, very broad, $CH_{2\,ax}$-calix and CH_2-arm); 3.86 (2 H, t, $J = 4.68$ Hz $CH_{2\,eq}$-calix), 3.40(4 H, broad) 3.20 (2 H, s), $CH_{2\,eq}$-calix); 2.0–2.8 (8 H, free H_2O); 1.59 (36 H, broad), 1.29 (6 H, semi-broad), 1.07 (2 H, d, $J_{H-P} = 5.72$ Hz), 0.90 (1 H, t, $J_{H-P} = 6.95$ Hz, $(CH_3)_2PO$; 1.15 (72 H, broad, H-*t*-Bu)). $^{31}P\{^1H\}$ NMR, 37.390, 37.392. $^{13}C\{^1H\}$ NMR, CH_3–P (14.95, 14.35); CH_2-ring (31.63); CH_2–P(74.38); CH (127.14).

2.3 Extraction procedure

The aqueous phases 1 (1 M HNO$_3$–0.5 M NaNO$_3$), 2, (1 M HNO$_3$–3.5 M NaNO$_3$), and 3, (3 M HNO$_3$–0.5 M NaNO$_3$) of UO_2^{2+} and/or trivalent rare-earth nitrates (RE = Y, La, Eu) were prepared as reported previously [6]. Organic phases of the calixarene were prepared in anhydrous chloroform. Organic phase 4: B_4bL^4 1.24 × 10^{-4} M; organic phase 5: B_4bL^4 3.27 × 10^{-4} M in order to maintain 1 : 1 and 1 : 2 metal-to-ligand ratios, respectively during the extraction process. The aqueous phase (5 cm^3) containing the metal salt(s) was poured into a high-quality glass vial fitted with a hermetic top; the corresponding organic B_4bL^4 phase (5 cm^3) was then added. The vial was capped and shaken at a speed of 300 rpm during 7 h at 291 ± 2 K. The vial was then kept still for 2 h to ensure optimum separation. When an emulsified phase formed between the organic and aqueous phases, the organic phase was slowly separated using a funnel; the combined aqueous and emulsified phases were filtered on a glass frit funnel (4–5.5 μm) under vacuum (1.33 Pa). The

added metal content of the aqueous and emulsified phases after filtration was always identical to that found in a portion of the aqueous phase before filtration. In general, the metal concentration was analyzed in each aqueous and organic phases before and after extraction by spectroscopic techniques, as described previously [6]. Extraction percentages: aqueous phase 1 and organic phase 4 (UO_2^{2+}: 28.01 ± 0.1, Eu: 14.0 ± 1.1, La: 3.0 ± 1, Y: 7.0 ± 0.1), organic phase 5 (UO_2^{2+}: 68.6 ± 0.2, Eu: 16.0 ± 1.2, La: 5.0 ± 1.0, Y: 9.0 ± 0.2); aqueous phase 2 and organic phase 4 (UO_2^{2+}: 32.7 ± 0.3, Eu: 0, La: 38.7 ± 1.1, Y: 5.60 ± 0.3), organic phase 5 (UO_2^{2+}: 76.1 ± 0.9, Eu: 0, La: 43.8 ± 1.1, Y: 23.5 ± 1.1); aqueous phase 3 and organic phase 4 (UO_2^{2+}: 11.3 ± 0.3, Eu: 0.20 ± 0.03, La: 0, Y: 0), organic phase 5 (UO_2^{2+}: 30.7 ± 0.5 Eu: 13.0 ± 1.0, La: 0, Y: 0).

2.4 Molecular modelling

MM3/CONFLEX/COSMO calculations

The structures were built and their minimum energies calculated using the CACHe Pro 5.02 program package for Windows® (Fujitsu Ltd., 2000–2001). Sequential application of Augmented MM3/CONFLEX procedures yielded the most stable conformers for compounds **1** and **2** and the free calixarene. Additionally, compound **1** and B_4bL^4 were simulated at 300 K by Dynamics using Augmented MM3 parameters. The calixarene structure has also been calculated by MOPAC/PM5 and MOPAC/PM5/COSMO procedures. COSMO evaluates the solvent effect in the stabilization of a structure and therefore the resulting calixarene structure was the base for the simulation of the actinide complexes. The MOPAC procedure could not be applied to the actinide complex molecules because it lacks parameters for 5*f*-elements.

Density functional (DFT) calculations on compound 1

These calculations were started with a MM (Molecular Mechanics) estimate by using the UFF (Universal Force Field) of CERIUS code [40]. DFT calculations were performed with the Amsterdam Density Functional code (ADF) [41] in vacuum. It solves numerically the Kohn-Sham equations of the system, employing different approximations to the electronic potential energy in the Local Density Approximation (LDA) and Generalized Gradient Approximation (GGA) types. A careful selection of the options was necessary. A total charge of 2.0 of the uranyl ion was considered for $[UO_2B_4bL^4(NO_3)(H_2O)]^{1+}$, and a spin polarized calculation was requested. The GGA PW91 potential was used. In order to have the best approach to the real uranyl complex molecule, the presence of uranium atom in the system was weighted by applying the ADF code introducing relativistic calculations. The ZORA scalar relativistic approximation was selected [42] and the corresponding atomic basis sets were of double-zeta (DZ) nature for H, C, U (with and without 5*d* shell), N, O, and P elements. The geometry was optimized using a Broyden–Fletcher–Goldfarb–Shanno (BFGS) method, until a minimal value for the energy gradient was obtained. During the calculations practical criteria have been used: (a) letting the DFT optimization run by several cycles and stopping it to use (as an intermediate step) a MM

calculation, employing as input the current geometry of the system and running again the DFT; (b) for selected ab initio calculations, the initial geometry was drawn by hand using the MM output. In any case, the gradients fluctuated significantly: the lowest the energy gradient was the largest the deviation of the uranyl bond angle (down to 147°) and the highest asymmetry of the molecule were. The most stable molecule was obtained for a gradient value of 0.06, a factor of 60 larger than the standard value (0.001).

2.5 Instrumental methods

IR spectra were measured on a PerkinElmer series 1600 IR spectrometer. UV-Vis and diffuse reflectance (DR) spectra were recorded on a PerkinElmer Lambda 10 spectrophotometer using 1-cm quartz cells and MgO pellets, respectively. Elemental analyses were performed on a Perkin Elmer 2400 series II (UAM-I, México) instrument. ^{1}H NMR, ^{31}P{^{1}H} NMR and ^{13}C{^{1}H} NMR spectra were recorded on a Bruker DMX500 spectrometer (500.13 MHz); chemical shifts δ are given with respect to TMS or CD$_3$CN or internal reference. Low-resolution emission and excitation spectra of solution samples were recorded at 291 and 77 K on a PerkinElmer LS-55 spectrofluorimeter in the range 200–900 nm. A 290-nm filter was used to minimize Rayleigh and Raman scatterings. Emission and excitation slits were set at 5 nm for frozen solutions and at 5, 7 or 10 nm for rt measurements. Excitation wavelengths (λ_{exc}) for measuring the emission spectra of the isolated uranyl calixarene complexes were selected based on the UV-Vis and excitation spectra of the free calixarene and uranyl salt solutions in acetonitrile; there are in line with those used in the literature [6, 9]: λ_{exc}(nm) = 270 for uranyl salt, 280 for free calixarene, 276 for **1** and 278 for **2**. Bulk frozen acetonitrile was measured using the same parameters than for frozen solutions of **1** and **2**, calixarene and uranyl salt in order to evaluate any interference due to scattered light, stray light or Raman transitions.

Solutions of the uranyl complexes and free calixarene ($\approx 2.2 \times 10^{-4}$ M) were prepared in spectroscopic grade acetonitrile inside a glove box. Lifetimes of the frozen solutions were measured on the same instrument; reported data are averages of at least five determinations. The emission spectra of uranyl nitrate in acetonitrile (5.08×10^{-4} and 5.10×10^{-3} M) were recorded at 291 and 77 K under the same experimental conditions as the uranyl complexes for testing the extent of energy transfer from the calixarene to the uranyl ion.

2.6 X-ray photoelectron spectroscopy (XPS)

The spectra were obtained with a THERMO-VG SCALAB 250 spectrometer equipped with an Al K_α X-ray source (1486.6 eV) and a hemispherical analyzer. The source was operated at 15 kV/150 W. The samples were introduced into the ultra high vacuum (UHV) chamber of the spectrometer (2.3×10^{-10} Torr) and measured at 297 K. The spot size in the beam was 500 μm. No rise of the pressure was observed during the analysis. The sample charging effect was compensated with controlled Argon flux isolating the samples in polyethylene terephthalate, the final vacuum was

2.3×10^{-8} Torr. A total of 30 scans were recorded for C$_{1s}$, O$_{1s}$, P$_{2p}$ peaks and 40 scans for U$_{4f}$ with energy step increment of 0.1 eV. Experimental peaks were decomposed into components using mixed Gaussian-Lorentzian functions and a non-linear squares fitting algorithm. Shirley background subtraction was applied. Binding energies were reproducible to within ± 0.2 eV and the C$_{1s}$ peak at 284.6 eV was used as a reference from adventitious carbon. Surface elemental composition was determined by fitting and integrating the U$_{4f}$, P$_{2p}$, O$_{1s}$ and C$_{1s}$ bands using theoretical sensitive factor provided by the manufacturer of the XPS apparatus.

3. Results and discussion

3.1 Isolation and characterization of the uranyl complexes

Reaction of B$_4$bL^4 with uranyl nitrates in stoichiometric ratios 1 : 1 in ethanol and 1 : 2 in acetonitrile yielded the following complexes: UO$_2$(NO$_3$)$_2$(B$_4$bL^4)$_n$·xH$_2$O ($n = 1$, $x = 2$, **1**; $n = 2$, $x = 6$, **2**) denoted UO$_2$(B$_4$bL^4)$_n$ below. Uranyl compounds are greenish. The UO$_2$(B$_4$bL^4)$_2$ complex is more hydrated than the UO$_2$(B$_4$bL^4) complex, a fact which can be traced back to the large affinity of the phosphinoyl groups for water [6, 36–38].

The vibrational spectra of complexes **1** and **2** reveal important features. One component of the P=O vibrations of free B$_4$bL^4, at 1172 cm^{-1}, disappears completely upon formation of the 1 : 1 complex, **1**, while the other component at 1196 is slightly red shifted (3 cm^{-1}). These changes imply that the four phosphinoylated arms of the calixarene are coordinated to uranyl in line with other works for actinide [6] and lanthanide [36, 37] complexes with phosphinoylated calixarenes. Bands attributable to ionic and monodentate nitrate anion as well as unbound and bound water molecules are present in the spectrum (see experimental section) which points to one monodentate nitrate anion and one water molecule coordinated to the uranyl ion since only two nitrates and two water molecules are present in **1**. So far this suggests that in this compound the coordination number (CN) of U(VI) ion is equal to 8 (six ligands and two uranyl oxygens) and CN = 6 for UO$_2^{2+}$.

In the 1 : 2 complex, **2**, both P=O bands observed in the free calixarene 1196, 1172, are slightly shifted (1194, 1173) with changes in their relative intensity which indicate the presence of coordinated and uncoordinated O=P groups in the complex. No bands assignable to coordinated nitrate or water molecules were found; therefore, it is assumed that three O=P arms per calixarene or four O=P arms of one calixarene and two of the other are coordinated to the uranyl ion, resulting in CN = 8 for U(VI).

The asymmetrical stretching frequency of the uranyl ion (ν_{asym} U–O), usually observed between 910 and 960 cm^{-1} is strongly affected by changes in the chemical environment [6, 43, 59]. The IR spectrum of uranyl nitrate hexahydrate (where two water molecules and two bidentate nitrates are coordinated) reveals this vibration as a very strong band at about 940 cm^{-1}. it is found as a strong band at 915 cm^{-1} in **1** and as a weak shoulder at ~ 916 cm^{-1} in **2**. It is interesting to note that in **2**, where no water molecules nor nitrate anions are bound to uranyl ion, the shifted band is a weak shoulder

while in **1** where apart from the calixarene, one monodentate nitrate and one water molecule are bound to uranyl, the band is still strong but 25 cm^{-1} red shifted. In both cases, these findings evidence the strong interaction of uranyl with the calixarene.

In the diffuse reflectance (DR) spectrum of the 1 : 1 complex, the $\pi \rightarrow \pi^*$(P=O) transition is blue shifted by 2825 cm^{-1} with respect to the free ligand, while the $\pi \rightarrow \pi^*$(C=C−phenyl) transition is red shifted by 2335 cm^{-1}. This further substantiates the P=O−metal cation interaction in the solid state complex, as well as the involvement of the calixarene scaffold to the stability of this complex. The spectrum of the 1 : 2 complex, **2** was less informative since the bands due to the $\pi \rightarrow \pi^*$ transition of uncoordinated OP bands mask partially those of the coordinated ones which cause its broadening. The $\pi \rightarrow \pi^*$ transition of the phenyl groups is only very slightly blue shifted (380 cm^{-1}).

3.2 Solution study

Acetonitrile was the best solvent for the solution studies of the isolated complexes **1** and **2** and the free calixarene since protic or aprotic solvents with lower polarities do not dissolve the complexes.

The UV-Vis spectra of B$_4$bL^4 and its complexes in acetonitrile display the main phenyl $\pi \rightarrow \pi^*$ ligand band in the range 275–279 nm. It is slightly red shifted (1–4 nm) in the complexes which additionally display a shoulder on the low-energy side (≈ 284 nm). Molar absorption coefficients of the 1 : 1 and 1 : 2 complexes were about 10 and 75% larger compared to the free calixarene ligand. In the corresponding complexes with B$_6$bL^6 [6], the increase in the molar absorption coefficients was about 10% larger with respect to **1** and **2**, indicating more influence of the metal centre on the electronic structure of the larger calixarene, in line with its better suited conformation for interacting with actinides [6]. Contributions to the differences between uranyl B$_4$bL^4 and B$_6$bL^6 complexes may come from differences in hydration and/or nitrate interaction.

It was demonstrated that in the 1 : 1 complex with B$_6$bL^6 no coordinated nitrates and/or coordinated water molecules are present, since the ligand fulfilled the maximum coordination number of U(VI) ion (CN=8) contrary to the 1 : 1 complex with B$_4$bL^4 where nitrate and water molecules are required. This somehow explains the lower molar absorption coefficients of **1**. In addition to the strong coordination ability of this calixarene towards uranyl, the affinity of uranium towards oxygen donors prevents de-coordination of nitrate or water molecule in acetonitrile.

The two partially coordinated calixarenes in compound **2** shield the uranyl ion from the medium, which influences the value of its molar absorption coefficient.

^{1}H-NMR spectra of 5×10^{-4} M solutions of B$_4$bL^4 and its uranyl complexes were recorded in CD$_3$CN at room temperature. The spectrum of complex **1**, which integrates for 88 protons (calixarene and two water molecules). The peaks assigned to Ar–CH_2–Ar, –CH_2–P(O) and $(CH_3)_2$P(O) are broad and shifted (± 0.1–0.2 ppm) with respect to those of the free calixarene [36]. In particular, the signals of the axial protons H$_{ax}$ of the methylene bridges and of the methylene linker of the phosphinoyl-derivatized arms collapse into a single broad resonance centred at 4.72 ppm after complexation, while the equatorial protons H$_{eq}$ give rise to a broad peak centred at 3.4 ppm. The broadened signals are typical of the presence of conformers in rapid equilibrium. Indeed, the methyl resonances of the $(CH_3)_2$P(O) and *t*-butyl groups appear as two signals, shifted to lower field and the other to higher field with respect to the free calixarene. We tentatively interpret this as arising from a species in which the four P=O groups are coordinated differently to the uranyl ion since the other signals are not split. The resonances of the aromatic protons and of the methylene bridges of the macrocycle are far less shifted than observed for the complexes with La^{III} [36] so that coordination of the ether O atoms can be ruled out. The spectrum of the 1 : 2 complex **2** revealed broader and more complex signals so that detailed interpretation had to be ruled out.

In order to get further insight into the solution properties of the complexes, luminescence spectra of uranyl complexes in acetonitrile at both 291 and 77 K were recorded. The excitation spectra of the two complexes (Fig. 2) display two main bands, one at 275 nm and the other at 225 nm, as well as a faint and broad feature centred at 325–330 nm, revealing both direct excitation into the uranyl ion (O $\rightarrow$ U LMCT) [16] and indirect excitation from the ligand (absorption spectrum, $\lambda_{max} = 275$ nm). The phosphorescence spectrum of UO$_2$(B$_4$bL^4) is displayed on Fig. 3 (top) and reveals the usual emission from lowest excited state of uranyl with five vibronic components at 495 (1), 516 (2), 540 (3), 564 (4, interfering with 2nd order Rayleigh scattering), and 593 (5) nm. Component 1 corresponds to the $E(0-0)$ transition, formally a magnetic dipole transition, which acquires appreciable electric dipole character for non-centrosymmetric environments [16, 44] it is red shifted by 13 nm with respect to uranyl nitrate, pointing to a sizeable uranyl-calixarene interaction.

In addition, a change of symmetry of the solvated uranyl cation (free uranyl in organic solvent) upon coordination to the calixarene (complexes) occurs since the intensity ratios of the vibronic bands are different with respect to [UO$_2$(B$_6$bL^6)]$^{2+}$ in which the inner coordination sphere only contains donor atoms from the calixarene. Vibronic bands are also broader (full width at half height, fwhh 7.7 *vs.* 6.5 cm^{-1}) [6] pointing to a more fluxional edifice. Since the main vibronic spacing for **1** at 291 K (857 cm^{-1}, see Table 1) is the same as the one found for the 1 : 1 complex with B$_6$bL^6, which has CN = 8, we postulate that **1** has also an 8-coordinate uranium centre in solution. The average vibronic spacing is related to the length of the O=U=O bond, r_{UO}, by the following equation [45]:

$$r_{UO} = 10\,650(\nu_{UO})^{-2/3} + 57.5\ [\text{pm}]$$

And for both 1 : 1 complexes with B$_4$bL^4 and B$_6$bL^6, $r_{UO} = 177.8$ and 178.6 pm, respectively are marginally longer than for the solvated uranyl ion, once more, in line with complexation by the calixarene. The emission spectrum of the 1 : 2 complex **2** is very similar to the phosphorescence spectrum of **1**, apart slight differences in the intensity ratios of the vibronic components (Fig. 3, Bottom), indicating a similar chemical environment around the uranium ion, as far as the inner coordination sphere is concerned (CN = 8 for both
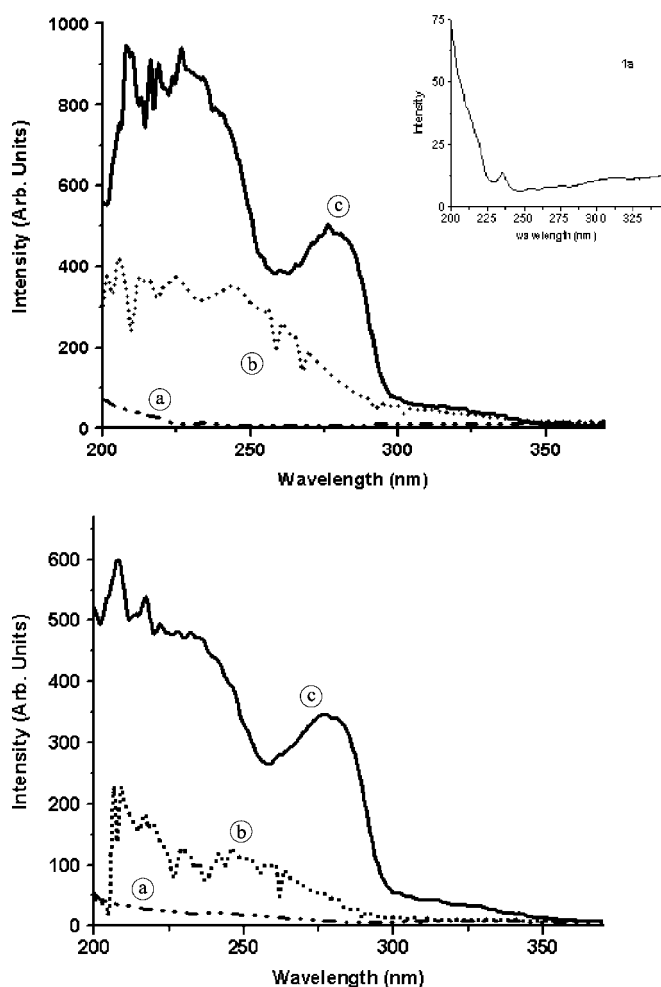
Fig. 2. Top: Excitation phosphorescence spectra of (a) 0.198 mM B_4bL^4, $\lambda_{emi} = 438$ nm, (b) 5.1 mM $UO_2(NO_3)_2 \cdot 6H_2O$, $\lambda_{em} = 485$ nm, (c) 0.347 mM $UO_2(NO_3)_2(B_4bL^4)$ $2H_2O$, **1**, $\lambda_{emi} = 495$ nm. Bottom: similar spectra for (a) 0.198 mM B_4bL^4, $\lambda_{emi} = 438$ nm, (b) 0.508 mM $UO_2(NO_3)_2 \cdot 6H_2O$, $\lambda_{em} = 485$ nm, (c) 0.198 mM $UO_2(B_4bL^4)_2(NO_3)_2 \cdot 6H_2O$, **2**, $\lambda_{emi} = 495$ nm. All spectra in frozen solutions of CH_3CN at 77 K.

complexes). $^1\Pi\Pi^*$ and $^3\Pi\Pi^*$ remaining emissions correspond to the coordinated calixarene ligands since no complete energy transfer from the ligand to uranyl occurs. The averaged uranyl-oxygen bond length calculated from the mean vibrational spacing is almost equal to the distance found for **1**, within experimental error, while the fwhh is somewhat narrower, 6.7 nm (Table 1), possibly indicating a more rigid coordination environment imposed by the two bound calixarenes and the absence of coordinated nitrate or water molecules.

Uranyl ion luminescent lifetimes are strongly dependent on the coordination environment. The luminescence decays for **1** and **2** in frozen acetonitrile are bi-exponential (Table 1). The corresponding lifetimes are very similar: a short lifetime (0.22–0.25 ms) accounting for $\approx 70\%$ of the emitted luminescence and a longer one (0.63–0.64 ms) representing $\approx 30\%$. An analogous situation with comparable lifetimes and populations has been reported for the complexes with B_6bL^6. Since the lifetime of un-complexed uranyl is much shorter ($< 2\,\mu s$, in organic solvents) [10] compared to complexed ones, and since the spectra of U(V) [46] and U(IV) [47] species are quite different, dis-
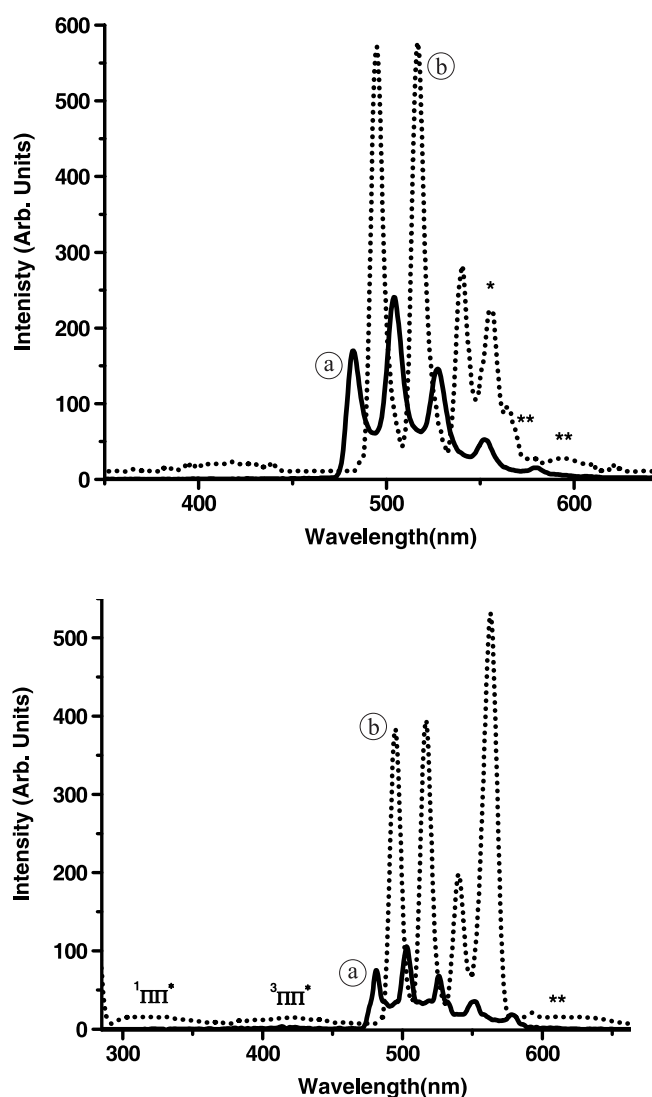

Fig. 3. Top: phosphorescence spectra of (a) 5.1 mM $UO_2(NO_3)_2 \cdot 6H_2O$, ($\lambda_{exc} = 270$ nm) and (b) 0.347 mM $UO_2(B_4bL^4)(NO_3)_2 \cdot 2H_2O$, ($\lambda_{exc} = 276$ nm) in frozen solutions of CH_3CN at 77 K; emission and excitation slits: 5 nm. Bottom: similar spectra for (a) 0.508 mM $UO_2(NO_3)_2 \cdot 6H_2O$, ($\lambda_{exc} = 270$ nm) and (b) 0.198 mM $UO_2(B_4bL^4)_2(NO_3)_2 \cdot 6H_2O$, $\lambda_{exc} = 278$ nm; filter 290 nm, emission and excitation slits: 7 nm. Stars denote second order Rayleigh scattering and double stars vibronic bands. $^1\Pi\Pi^*$ (singlet excited state) and $^3\Pi\Pi^*$ (triplet excited state.).

sociation of the complexes and reduction of uranyl can be ruled out; moreover, hydroxo species display much larger fwhh and can also be excluded [6]. Therefore, the bi-exponential decays reflect equilibria between two complexed species, possibly featuring different conformations of the calixarenes, one conformation being more "protective" than the other, leading to a longer lifetime.

3.3 X-photoelectron spectroscopy of uranyl complexes

The extent of the covalent and/or ionic character of the bonding, the coordination geometry and coordination numbers, among others, determine the binding energies (BE) of the uranyl orbitals [48, 49]. Therefore, XPS spectra of complexes **1** and **2** were recorded and are displayed on Figs. 4 and 5, respectively. Relevant parameters are listed in Table 2.

Table 1. Main luminescence parameters of uranyl and uranyl calixarene complexes in acetonitrile extracted from phosphorescence spectra.

Compd.	$E(0-0)/$ cm^{-1}	Intensity ratio, I_n/I_1		Mean vibronic spacing $(\nu_{UO})/$ cm^{-1a}		$R_{U-O}/$ pm^b	FWHH/ nm	Lifetimes/μs (% species)
	77 K	77 K	291 K	77 K	291 K	77 K	77 K	77 K
$[UO_2]^{2+c}$	20 780	1.40; 0.91; 0.47; 0.25	1.34; 0.88; 0.43; 0.20	875(24)	840(47)	173.9	10.5	2 ± 0.1^d
1	20 200	0.99; 0.45; 0.15; 0.05	0.97; 0.73	834(31)	857(12)	177.8	7.7	220 ± 10 (73) 640 ± 100 (27)
2	20 210	0.97; 0.53; 0.08; 0.06	1.0; 0.66	846(33)	840(10)	176.6	6.7	250 ± 30 (71) 630 ± 110 (29)

a: Standard deviation (2σ) in parentheses; b: see text; c: in dry acetonitrile, this work; d: at room temperature, from Ref. [10].
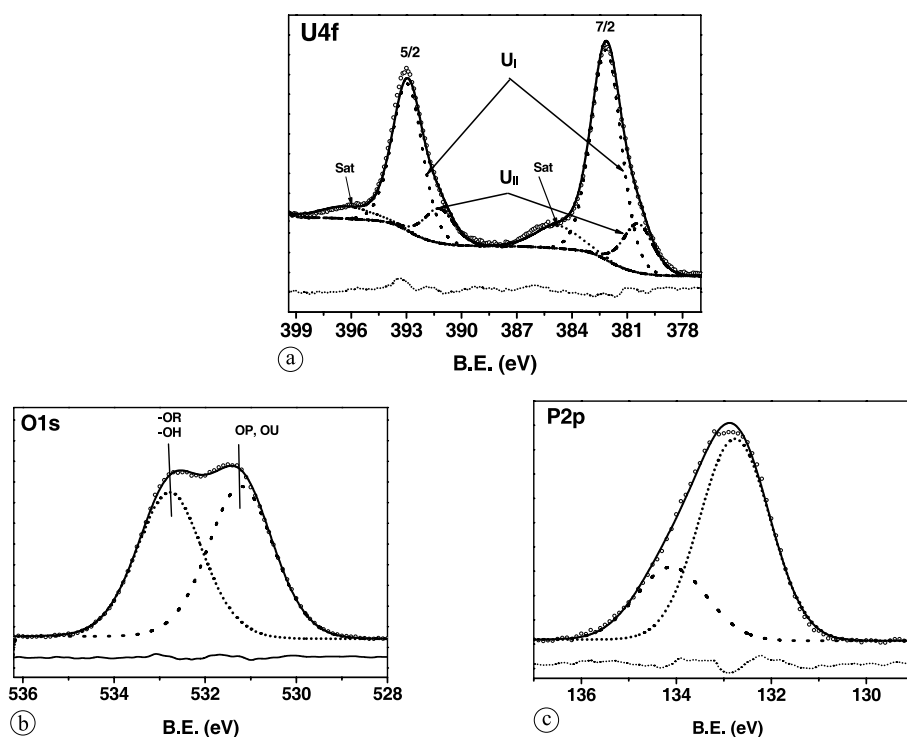
Fig. 4. XPS spectra of $UO_2(B_4bL^4)(NO_3)_2\cdot$ $2H_2O$.

Before interpreting these data, we stress the fact that all of the analytical tools used so far have demonstrated the purity and stability (*e.g.* heating the KBr pellets did not alter the samples) of the complexes under investigation. High-vacuum treatment at room temperature led to removing the lattice water molecules but not the bonded ones. Irradiation times shorter than 15 min were used for XPS measurements in order to prevent the reduction of uranyl to lower oxidation state [48, 50, 51]. In addition, B_4bL^4 is neutral and the P=O donors are linked to methyl groups which are less electron-donating substituents than phenyl groups, so that uranyl reduction as observed with $OP(Phe)_3$ is unlikely to occur [51].

U(4f) spectra

For both compounds, the uranium spectra reveal two broad peaks, $U(4f_{7/2})$ and $U(4f_{5/2})$, separated by 10.8 eV and featuring shoulders on both sides. The spectra have been deconvoluted into Gaussian-Lorentzian functions and the best

fit yielded two main and well defined bands each flanked by a broad and weak shake-up satellite on the high binding energy side and a well defined small band on the low-energy side. The two $U(4f_{5/2;7/2})$ doublets are labelled U_I and U_{II}. The major one represents 81 and 74% of the bulk U concentration for **1** and **2**, respectively. In the case of $U(4f_{7/2})$ the U proportions on the surface of the samples have also been measured and found to be the same as for the bulk sample (4 : 1 and 3 : 1 ratios for **1** and **2**, respectively). Binding energies (BE) are quasi identical for both complexes, except $U_{II}(4f)$ which is 0.3 eV larger in **2**, while the full width at half height of all four peaks are the same. Some differences are seen between **1** (Fig. 4a) and **2** (Fig. 5a) with respect to the energies of the satellites, ΔE_I(sat) being equal to 2.75 ($J = 7/2$) and 3.05 eV ($J = 5/2$) for **1** compared to 3.52 and 3.31 eV for **2**; similar data for ΔE_{II}(sat) are 4.75 and 4.78 eV (**1**) and 5.04 and 4.83 eV (**2**). The position of the satellite peak with respect to the photoelectron peak depends on the energy difference between the ground state and the higher orbital to which the valence electrons of ura-

Table 2. Selected binding energies (BE) of uranium, oxygen, and phosphorus together with the percentages of uranium atoms on the surface (I_S) and in the sample (I).[a]

Levels	$UO_2(NO_3)_2(B_4bL^4)\cdot 2H_2O$		$UO_2(NO_3)_2(B_4bL^4)_2\cdot 6H_2O$	
	BE/eV; I_S, I (%), or Δsat/eV	FWHH/ eV	BE/; I_S, I (%), or Δsat/eV	FWHH/ eV
$U_I\,4f_{7/2}$	382.1; *5.2, 81.1*	2.0	382.2; *2.8, 73.6*	2.0
$U_{II}\,4f_{7/2}$	380.4; *1.2, 18.9*	2.0	380.7; *1.0, 26.4*	2.0
$\Delta U_I\,4f_{7/2}$ (sat)	*2.8*		*3.5*	
$\Delta U_{II}\,4f_{7/2}$ (sat)	*4.8*		*5.0*	
$U_I\,4f_{5/2}$	392.9	2.0	393.0	2.0
$U_{II}\,4f_{5/2}$	391.2	2.0	391.5	2.0
$\Delta U_I\,4f_{5/2}$ (sat)	*3.05*		*3.3*	
$\Delta U_{II}\,4f_{5/2}$ (sat)	*4.8*		*4.8*	
O_{1s}	531.2/532.8	1.8	530.9/532.6	1.8
P_{2s}	132.8/134.1	1.7	132.5/133.8	1.7

a: Experimental conditions: spots diameter $= 500\,\mu m$; 15 kV, 150 W.
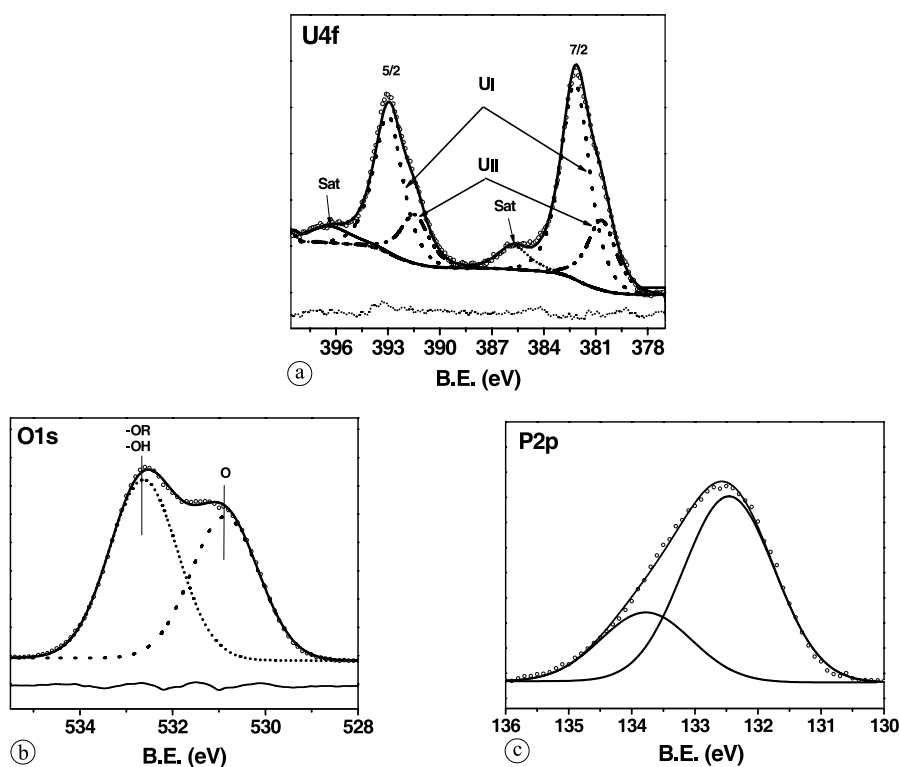
Fig. 5. XPS spectra of $UO_2(B_4bL^4)_2(NO_3)_2\cdot 6H_2O$.

nium are excited, the valence of the elements and the type and number of its nearest-neighbours [48, 49]. In particular, ΔE(sat) tends to decrease with increasing covalent character of the U-ligand bonds [52]. Reported average ΔE(sat) values are 4.0 (2.4–4.5), 6.6 (6–7), and 8 (7.8–8.5) eV for uranyl, U(IV), and U(V) compounds respectively [48–50, 52, 53]. Although binding energy differences are larger than 4 eV for U_{II}, they are well below 6 eV, so that we infer that no reduction occurred in the samples, particularly in view of the other evidences reported above. The satellite features depend on the bonding environment and could therefore also be useful in estimating the covalent/ionic character of the U-ligand bonds; however a precise correlation is not presently at hand [50].

Moreover, binding energies for various oxidation states are often very close to each other. For instance, in the uranium mineral brannerite, two U(VI) species in different structural environments were identified, which give rise to two bands at 381.4, and 382.1 eV, while another band at 380.6 eV was assigned to U(V). Furthermore, in Na-substituted metaschoepite a band at 380.5 eV was assigned to U(IV). This demonstrates that there is a narrow border-line between the U(4f) bonding energies of different oxidation numbers. On the other hand, two different U(VI) species were identified in this material characterized by U(4$f_{7/2}$) bands at 381.3 and 382.1 eV [48]. Regarding the effect of X-ray irradiation, an exposure of several hours of metaschoepite only induced 5% reduction of U(VI) [48] while a 15-minute exposure of U(VI) deposited on mica did not produce enough reduced species to be detected [50]. The second set of signals is consequently assigned to a different coordination environment for the uranium ions. Ligand

B_4bL^4 has a cone conformation in acetonitrile which is retained in its lanthanide complexes. However, luminescence studies of the uranyl complexes in frozen acetonitrile solutions revealed the presence of two structurally different species possibly differing by the calixarene conformation. It is noteworthy that the proportion of the emitting species with the longer lifetime, $\approx 30\%$ (Table 1) is in reasonably good agreement with that associated with U_{II} (19–26%), especially given the fact that the medium is different (frozen solution *vs.* solid state).

O_{1s} and P_{2p} spectra

Spectra of the O_{1s} and P_{2p} levels are broad, the former revealing two resolved maxima while the latter are asymmetric on their high-energy side. The best fit in the deconvolution of the O_{1s} spectrum (Figs. 4b and 5b) yielded two peaks with different intensities and FWHH = 1.8 eV. In addition to uranyl oxygen atoms, both complexes **1** (Fig. 4b) and **2** (Fig. 5b) have several types of oxygen atoms, phosphoryl and ether groups from the calixarene molecules, nitrate and water molecules. It has recently been demonstrated that the nature of ligands influence the BE of uranyl oxygen atoms. In most compounds reported to date $BE(O_{1s})$ lies in the range 530.8–532.4 eV (FWHH ≈ 2 eV); exceptions are nitrate salts $MUO_2(NO_3)_3$ (M = Cs, Rb) and $UO_2(NO_3)_2 \cdot 2H_2O$ (533.6–533.9 eV, one peak reported) while the oxide $CaUO_2O_2$ has $BE(O_{1S})$ = 530.2 eV [49, 52]. We note that in uranium minerals, interstitial water and hydroxyl groups have $BE(O_{1s})$ in the range 532.1–533.8 eV [49]. Therefore, we assign the bands centred at 531.2 and 530.9 eV to uranyl oxygen atoms and phosphoryl oxygen atoms [54–56], while those centred at 532.8 and 532.6 eV correspond to the other oxygen atoms (phenoxy-, nitrate, water) for compounds **1** and **2**, respectively. The higher energy band in the O_{1s} spectrum of **1** (Fig. 4b) is less intense compared to **2** (Fig. 5b), which would be consistent with the smaller content of lattice water.

Similarly to the O_{1s} spectra, the P_{2p} bands of **1** (Fig. 4c) and **2** (Fig. 5c) can be de-convoluted into two components with different intensities. The BE of phosphorus in O=P groups coordinated to uranyl is affected by the U−OP bond strength. A stronger coordination of U−OP means significant PO → U electron transfer, then the photoelectron energy of P_{2p} increases. The more intense band at 132.8 eV (**1**) and 132.5 eV (**2**) is therefore associated with a less strong U−OP bond in a complex with the less stable conformation while the less intense band at 134.1 (**1**) and 133.8 eV(**2**) is associated with a stronger and shorter U−OP bond.

3.4 Molecular modelling

In order to substantiate the experimental results described above, model calculations have been performed both in vacuo and in a polar solvent on the free calixarene and on the actinide complexes. Surprisingly, the predominant low-energy isomer calculated for B_4bL^4 was a 1,3 alternate conformer, even in highly polar water, while in less polar solvents such as $CHCl_3$ and CH_3CN, NMR data are consistent with a cone conformation. Such conformation was also

found for the acetonitrile adduct of this calixarene in the solid state by X-ray crystallography [36].

The structural versatility of actinide complexes in solution and solid arises from the lack of strong crystal field effects for the $5f$ electronic configurations as well as from their large ionic radii. The predominant ionic character of the bonding leads to a wide variety of coordination numbers (CN) and symmetries. The uranyl ion is usually restricted to CN = 4–6 [1, 13, 16, 57, 58]. For CN = 6, due to the linearity of UO_2^{2+}, the six donor atoms are usually located in the equatorial plane, but it is also common that a distorted hexagonal bipyramidal polyhedron be found with the six donor atoms arranged in a puckered fashion.

Modelled uranyl calixarene molecules with AugMM3/ CONFLEX at vacuum or AugMM3/dynamics calculations at 300 K revealed U–OP, U–OH_2 and NO_2–U lengths in the ranges reported for similar complexes containing these types of donors (2.3–2.7 Å) but the uranyl bond angles (*e.g.* 169° for **1**, 126° for **2**) were out of the accepted range for a hexacoordinate uranyl complex (176–180°) [13, 16, 57, 58]. The modelling was based on the experimental data, therefore the structures of **1** and **2** were built for uranyl in a hexacoordinate geometry.

The structure of **1**, a monocationic complex $[UO_2B_4bL^4(NO_3)(H_2O)]^{1+}$ has four OP arms, one monodentate nitrate and one water molecule coordinated to uranyl. Its molecular modelling yielded structural parameters as U−OP bond lengths, U−O=P bond angles varying from one coordinated OP arm to the other, pointing to four OP arms in an unsymmetrical arrangement around the uranyl in agreement with the spectroscopic results. For the structure of **2**, a bicationic complex $[UO_2(B_4bL^4)_2]^{2+}$ was modelled in two arrangements: (i) with 4 OP arms of one calixarene and two of the other bound to the uranyl, and (ii) with three OP arms from each calixarene. In both cases, the minimum energy was high. Therefore, considering the affinity of water towards OP groups and the presence of six water molecules in **2**, water molecules were linked to each one of the free OP arms. The most stable structure was that of three OP arms per calixarene coordinated to uranyl where the free OP of each calixarene was linked to one water molecule by weak bonding simulating hydrogen bonding. This reduced three times the mobility of the complex. Both calixarenes are located in the first coordination sphere of the uranyl and hydrogen bonded to water molecules, thus the structure of the complex can be written as $[H_2O \cdots B_4bL^4 \rightarrow UO_2 \leftarrow B_4bL^4 \cdots H_2O]^{2+}$.

In spite of the flaw concerning the O=U=O bond angle, the modelling reflects an 8-coordinate U(VI) ion in both complexes in agreement with the experimental results.

DFT calculations were attempted on complex **1** in order to find a more realistic O=U=O angle bond. The standard uranyl valence configuration $7s5f6d$ was found to be the most adequate for the ab initio calculations including relativistic effects, which yielded an optimized molecule in which the linearity of uranyl is practically maintained but not the U−O bond length of uranyl. In fact, the O−U−O angle found (178.8°) is comparable to the one for uranyl complexes with phosphoryl [59] and nitrate [60] donors (177–180°) but which are highly asymmetric. Several fac-

tors exert symbiotic effects leading to this asymmetry: the size of the calixarene which does not permit complete inclusion of the uranyl cation, steric and electronic restrictions due to the linear geometry of uranyl, the mono-coordinate mode of nitrate, and coordinated water molecules. The found geometrical parameters associated with the calculated coordination polyhedron of **1** like U$-$OP bond lengths, PO$-$U$-$OP bond angles and dihedral angles do not allow us to propose the modeled molecule by DFT as the representative of compound **1**. Further interpretation was therefore not conducted.

3.5 Liquid–liquid extraction

Generally speaking, actinide cations are much better extracted than rare earths by phosphinoylated calixarenes, which has been encouraging in the perspective of An/Ln separation in liquid–liquid or liquid–solid systems [6, 22–31]. Therefore, in this work, the extraction ability of B_4bL^4 towards UO_2^{2+}, Y(III), La(III), and Eu(III) ions was also tested. The study was performed using three different aqueous nitric phases (aqueous phases 1, 2 and 3, see experimental) and two different calixarene concentrations in chloroform corresponding to metal : ligand ratios of ≈ 1 (organic phase 4) and ≈ 2.5 (phase 5). It was found that increasing the concentration of the calixarene by a factor 2.5 in going from organic phase 4 to phase 5 leads to a concomitant increase in the extraction of the uranyl cations (average increase is > 2.3-fold), in line with the formation of 1 : 2 complexes discussed above. Increasing the concentration of nitric acid in the aqueous phase from 1 to 3 M is quite detrimental to uranyl extraction (see experimental) and blocks lanthanum and yttrium ion extraction. On the other hand, boosting sodium nitrate concentration from 0.5 to 3.5 M, the uranyl extraction is not substantially increased but its distribution ratio goes from 0.53 to 1.90. However, the increase in nitrate concentration gives rise to a remarkable improvement in La^{3+} extraction, by a factor ≈ 10 while Eu^{3+} extraction drops to 0. It has been recently demonstrated that the salting-out effect plays an important role in La^{3+} extraction with calix[6]arene B_6bL^6 [6]. In fact, the behaviour of B_4bL^4 as extractant for rare earths is similar to that found for the *p-tert*-butylcalix[4]arene derivative containing diphenyl-phosphinoyl groups [25] and others [26, 30]. B_4bL^4 has also proved to be useful as a synergistic agent in the solvent extraction of lanthanides with a pyrazolone derivative [39].

It has been found [6] that the calixarene concentration required for determining the stoichiometry of the extracted species has to be much larger than 3×10^{-4} M (up to approx. 1×10^{-3} M, in $CHCl_3$). In the present work, extraction of uranyl with more concentrated calixarene solutions did not give good results due to an emulsion formed between the organic and aqueous phases so that a suitable graphic to evaluate the number of calixarene molecules bound to uranyl could not be built. However, extracted species with two predominant stoichiometries: 1 M : 1 L and 1 M : 2 L have been reported for similar phosphinoylated calixarenes in chloroform [6] and in m-nitrobenzotrifluoride [30]. According to the extraction behaviour of uranyl in presence of B_4bL^4, it is anticipated that a 1 : 1 species was extracted.

4. Conclusions

The tetra-phosphinoylated *p-tert*-butylcalix[4]arene forms stable uranyl(VI) complexes with 1 : 1 and 1 : 2 stoichiometries in organic media. A combination of several experimental analytical techniques and theoretical modelling leads to the conclusion that coordination numbers for U(VI) ion are most probably 8 in these edifices. The uranyl complexes display enhanced luminescence and longer lifetimes due to the complexation, which allows <u>one</u> <u>to</u> get information on the solution composition: for both stoichiometries, lifetime data point to the existence of two different species in solution featuring different conformations of the calixarene, as pointed out by molecular modelling. These species also exist in the solid state as proved by XPS data. It is noteworthy that the proportion of the emitting species with the longer lifetime (27–29%) is in reasonably good agreement with that associated with U_{II} (19–26%), especially given the fact that the medium is different (frozen solution *vs.* solid sate). Therefore, it is proposed that for **1** and **2**, in solid and in solution, the U(VI) central ion is in an 8-coordinate geometry.

The B_4bL^4 calixarene is a reasonably good extractant for uranyl(VI) ions but a poor one for rare earths. Furthermore, the extraction behaviour and separation ability is much dependent on the initial conditions, pH and nitrate concentration, so that modulation of the extraction process is easy. Further study on these systems using more lipophilic macrocyclic receptors in which the wider rim of the calixarene is decorated with octyl substituents is in progress.

References

1. Cotton, S.: *Lanthanide and Actinide Chemistry*. 1st Edn., John Wiley & Sons Ltd., Chichester (2006).
2. Mishra, S.: Coord. Chem. Rev. **252**, 1996 (2008).
3. Sutton, A. D., John, G. H., Sarsfield, M. J., Renshaw, J. C., May, L., Martin, L. R., Selvage, A. J., Collison, D., Helliwell, M.: Inorg. Chem. **43**, 5480 (2004).
4. Billard, I.: Lanthanide and actinide solution chemistry as studied by time-resolved emission spectroscopy. In: *Handbook on the Physics and Chemistry and Rare Earth.* (Gschneidner Jr., K. A., Bünzli, J.-C. G., Pecharsky, V. K., eds.) Elsevier Science B. V., Amsterdam (2003).
5. Thuery, P., Nierlich, M., Masci, B., Asfari, Z., Vicens, J.: J. Chem. Soc., Dalton Trans. 3151 (1999).
6. Ramirez, F. d. M., Varbanov, S., Padilla, J. P., Bünzli, J.-C. G.: J. Phys. Chem. B **112**, 10976 (2008).
7. Choppin, G. R., Rizkalla, E. N.: Solution chemistry of actinides and lanthanides. In: *Handbook on the Physics and Chemistry of Rare Earths.* (Gunzler, H., Eyring, L., Choppin, G. R., Lander, G. H., eds.) Elsevier Science Publ. B.V., Amsterdam (1994).
8. Edelstein, N. M.: J. Alloys Compd. **223**, 197 (1995).
9. Moulin, C., Laszak, I., Moulin, V., Tondre, C. : Appl. Spectrosc. **52**, 528 (1998).
10. Darmanyan, A. P., <u>Khudyakov</u>, I. V.: Photochem. Photobiol. **52**, 293 (1990).
11. Servaes, K., De Houwer, S., Görller-Walrand, C., Binnemans, K.: Phys. Chem. Chem. Phys. **6**, 2946 (2004).
12. De Houwer, S., Servaes, K., Görller-Walrand, C.: Phys. Chem. Chem. Phys. **5**, 1164 (2003).

13. Umeda, K., Zukerman-Schpector, J., Isolani, P. C.: Polyhedron **25**, 2447 (2006)
14. Zucchi, G., Maury, O., Thuery, P., Gumy, F., Bünzli, J.-C. G., Ephritikhine, M.: Chem. Eur. J. **15**, 9686 (2009).
15. Denning, R. G.: Properties of the $UO_2{}^{n+}$ ($n = 1, 2$) ions. In: *Gmelin's Handbook of Inorganic Chemistry "U"*. (Fluck, E., ed.) Springer Verlag, Berlin (1983), A6, Sect. 2, p. 31.
16. Denning, R. G.: J. Phys. Chem. A **111**, 4125 (2007).
17. Wiebke, J., Moritz, A., Cao, X., Dolg, M.: Phys. Chem. Chem. Phys. **9**, 459 (2007).
18. Schlosser, F., Kruger, S., Rosch, N.: Inorg. Chem. **45**, 1480 (2006).
19. Wiebke, J., Moritz, A., Glorius, M., Moll, H., Bernhard, G., Dolg, M.: Inorg. Chem. **47**, 3150 (2008).
20. Boulet, B., Joubert, L., Cote, G., Bouvier-Capely, C., Cossonnet, C., Adamo, C.: Inorg. Chem. **47**, 7983 (2008).
21. Baaden, M., Berny, F., Muzet, N., Troxler, L., Wipff, G.: In: *Calixarenes for Separations*. (Lumetta, G. J., Rogers, R. D., Galopan, A. S., eds.) ACS Symposium Series No. 757, Am. Chem. Soc., Washington, D.C. (2000), Chapt. 6, p. 71ff.
22. Sliwa, W., Girek, T.: J. Inclus. Phenom. Macrocycl. Chem. **66**, 15 (2010).
23. Mokhtari, B., Pourabdollah, K., Dallali, N.: J. Radioanal. Nucl. Chem. **287**, 921 (2011).
24. Mokhtari, B., Pourabdollah, K., Dallali, N.: J. Inclus. Phenom. Macrocycl. Chem. **69**, 1 (2011).
25. Yaftian, M. R., Burgard, M., Matt, D., Dieleman, C. B., Rastegar, F.: Solv. Extr. Ion Exch. **15**, 975 (1997).
26. Arnaud-Neu, F., Browne, J. K., Byrne, D., Marrs, D. J., McKervey, M. A., O'Hagan, P., Schwing-Weill, M.-J., Walker, A.: Chem. Eur. J. **5**, 175 (1999).
27. Arnaud-Neu, F., Barboso, S., Byrne, D.: In: *Calixarenes for Separations*. (Lumetta, G. J., Rogers, R. D., Galopan, A. S., eds.) ACS Symposium Series No. 757, Am. Chem. Soc., Washington, D.C. (2000), Chapt. 12, p. 150ff.
28. Alexandratos, S. D., Natesan, S.: Ind. Eng. Chem. Res. **39**, 3998 (2000).
29. Asfari, Z., Böhmer, V., Harrowfield, J. M., Vicens, J., Saadioui, M. (eds.): *Calixarenes 2001*. Kluwer Academic Publishers, Dordrecht, Boston, London (2001).
30. Karavan, M., Arnaud-Neu, F., Hubscher-Bruder, V., Smirnov, I., Kalchenko, V.: J. Inclus. Phenom. Macrocyc. Chem. **66**, 113 (2010).
31. Talanova, G. G.: Ind. Eng. Chem. Res. **39**, 3550 (2000).
32. Galletta, M., Baldini, L., Sansone, F., Ugozzoli, F., Ungaro, R., Casnati, A., Mariani, M.: Dalton Trans. **39**, 2546 (2010).
33. Hall, I., Nicholson, G. P., Piper, T. J., Tay, D. M., Williams, D. R.: Radiochim. Acta **69**, 225 (1995).
34. Ramirez, F. d. M., Charbonnière, L. J., Muller, G., Scopelliti, R., Bünzli, J.-C. G.: J. Chem. Soc., Dalton Trans. 3205 (2001).
35. Ramirez, F. d. M., Charbonnière, L. J., Muller, G., Bünzli, J.-C. G.: Eur. J. Inorg. Chem. 2348 (2004).
36. Le Saulnier, L., Varbanov, S., Scopelliti, R., Elhabiri, M., Bünzli, J.-C. G.: J. Chem. Soc., Dalton Trans. 3919 (1999).
37. Ramirez, F. d. M., Varbanov, S., Cécile, C., Muller, G., Fatin-Rouge, N., Scopelliti, R., Bünzli, J.-C. G.: J. Chem. Soc., Dalton Trans. 4505 (2002).
38. Puntus, L. N., Chauvin, A.-S., Varbanov, S., Bünzli, J.-C. G.: Eur. J. Inorg. Chem. 2315 (2007).
39. Atanassova, M., Lachkova, V., Vassilev, N., Varbanov, S., Dukov, I.: J. Inclus. Phenom. Macrocycl. Chem. **58**, 173 (2007).
40. CERIUS², Accelrys Software Inc., San Diego, CA, USA (2010).
41. Te Velde, G., Bickelhaupt, F. M., Baerends, E. J., Fonseca Guerra, C., Van Gisbergen, S. J. A., Snijders, J. G., Ziegler, T.: J. Comput. Chem. **22**, 931 (2001).
42. van Lenthe, E., Ehlers, A., Baerends, E. J.: J. Chem. Phys. **110**, 8943 (1999).
43. Nakamoto, K.: *Infrared and Raman Spectra of Inorganic and Coordination Compounds. Part A. Theory and Applications in Inorganic Chemistry*. John Wiley Interscience Publ., New York (1997).
44. Burrows, H. D., Miguel, M. D.: Adv. Colloid Interface Sci. **89**, 485 (2001).
45. Bartlett, J. R., Cooney, R. P.: J. Mol. Struct. **193**, 295 (1989).
46. Grossmann, K., Arnold, T., Ikeda-Ohno, A., Steudtner, R., Geipel, G., Bernhard, G.: Spectrochim. Acta A **72**, 449 (2009).
47. Kirishima, A., Kimura, T., Nagaishi, R., Tochiyama, O.: Radiochim. Acta **92**, 705 (2004).
48. Schindler, M., Hawthorne, F. C., Freund, M. S., Burns, P. C.: Geochim. Cosmochim. Acta **73**, 2471 (2009).
49. Schindler, M., Hawthorne, F. C., Freund, M. S., Burns, P. C.: Geochim. Cosmochim. Acta **73**, 2488 (2009).
50. Ilton, E. S., Boily, J. F., Bagus, P. S.: Surf. Sci. **601**, 908 (2007).
51. Duval, P. B., Kannan, S.: J. Alloys Compd. **444**, 673 (2007).
52. Teterin, A. Y., Teterin, Y. A.: Russ. Chem. Rev. **73**, 541 (2004) [Engl. translation].
53. Ilton, E. S., Haiduc, A., Cahill, C. L., Felmy, A. R.: Inorg. Chem. **44**, 2986 (2005).
54. Bourbigot, S., Le Bras, M., Delobel, R., Gengembre, L.: Appl. Surf. Sci. **120**, 15 (1997).
55. Jalil, P. A., Faiz, M., Tabet, N., Hamdan, N. M., Hussain, Z.: J. Catal. **217**, 292 (2003).
56. Ignatova, M., Manolova, N., Lachkova, V., Varbanov, S., Rashkov, I.: Macromol. Rapid Commun. **29**, 1871 (2008).
57. Deshayes, L., Keller, N., Lance, M., Navaza, A., Nierlich, M., Vigner, J.: Polyhedron **13** 1725 (1994).
58. Thuery, P., Keller, N., Lance, M., Vigner, J. D., Nierlich, M.: New J. Chem. **19**, 619 (1995).
59. de Aquino, A. R., Bombieri, G., Isolani, P. C., Vicentini, G., Zukerman-Schpector, J.: Inorg. Chim. Acta **306**, 101 (2000).
60. Caville, C., Poulet, H.: J. Inorg. Nucl. Chem. **36**, 1581 (1974).